Available online at www.sciencedirect.com

Chemical Engineering Research and Design

journal homepage: www.elsevier.com/locate/cherd

Separation of nanoplastics from synthetic and industrial wastewater using electrolysis-assisted flotation approach: A green approach for real-time contaminant mitigation

Vishal Singh Pawak[a], Chandra Shekhar[a], Vijay A. Loganathan[b], Manigandan Sabapathy[a,*]

[a] Department of Chemical Engineering, Indian Institute of Technology Ropar, Rupnagar 140001, Punjab, India
[b] Department of Civil Engineering, Indian Institute of Technology Ropar, Rupnagar 140001, Punjab, India

ARTICLE INFO

Article history:
Received 3 June 2023
Received in revised form 16 August 2023
Accepted 22 August 2023
Available online 25 August 2023

Keywords:
Nanoplastics
Polystyrene waste
Electrolysis
Wastewater
Flotation
Removal efficiency

ABSTRACT

Nanoplastics pose a significant global environmental concern, as they can accumulate emerging pollutants and enter the food chain, endangering human health and ecosystems. Wastewater treatment plants (WWTPs) have been identified as the primary source of micro and nanoplastic contamination, necessitating the development of effective removal methods. This study investigates the efficacy of electrolysis-assisted flotation (EF) process for removing nanoplastics from synthetic wastewater, using polystyrene-type nanoparticles synthesized from expanded polystyrene waste (EPS) as representative nanoplastic contaminants. Electrolysis experiments were conducted using parallel aluminium electrodes under low-voltage conditions. The study systematically explores the influence of various process parameters, including electrode spacing, salt concentration, nanoplastics concentration, and applied voltage, on the removal efficiency of nanoplastics. The removal efficiency was evaluated using a turbidity meter and dynamic light scattering technique. The derived count rate (DCR) obtained from dynamic light scattering supplements the nephelometric turbidity units (NTU) and provides a reliable estimate of the nanoplastics sample concentration. Under optimized conditions, with a specified electrolyte concentration and pH of 7.2 ± 0.3, the EF process achieved an impressive removal efficiency of nearly 95 % (94 % per DCR). A notable advantage of the proposed method is forming a foamy layer on top of the reactor when nanoplastics and coagulants are mixed, facilitating easy removal by simple scraping. This study provides valuable insights into developing an eco-friendly and sustainable approach for the large-scale removal of nanoplastics. The results contribute to advancing wastewater treatment strategies and addressing the pressing issue of nanoplastic pollution.

* Corresponding author.
E-mail address: mani@iitrpr.ac.in (M. Sabapathy).

https://doi.org/10.1016/j.cherd.2023.08.038
0263-8762/

1. Introduction

The extensive use and exponential production growth of plastic have led to a surge in industrial plastic waste, resulting in the ubiquitous presence of microplastics and nanoplastics in the environment (Picó et al., 2022). Researchers predict oceans will contain more plastic than fish, and 99 % of seabirds may ingest it. The personal care and cosmetic industries generate the most waste, causing potential threats to land and aquatic environments, with 93 % of waste linked to polyethylene-derived beads (Gouin et al., 2015). These emerging contaminants fragment into tiny nanoplastics, which become nanoplastics ranging in size from 1 nm to 1000 nm over time due to UV degradation, mechanical stress, and biological processes. (Napper and Thompson, 2019; Dawson et al., 2018; Geyer et al., 2017; Bianco et al., 2020; Bond et al., 2018).

The ubiquitous presence of microplastics and nanoplastics in various environmental compartments, including water sources, poses a severe threat to aquatic life and human health as they can accumulate in living organisms and eventually enter the food chain (Erni-Cassola et al., 2019). Conventional treatment processes used in wastewater treatment plants (WWTPs) are ineffective in removing these particles, making WWTPs one of the primary sources of microplastics and nanoplastics in the environment (Li et al., 2020). Therefore, developing efficient techniques to remove these particles from wastewater is essential to protect the environment, and public health (Zeng, 2018).

Several studies have reported the successful removal of nanoplastics from simulated wastewater through coagulation and electrocoagulation. For instance, (Chen et al., 2020) investigated the sedimentation of polystyrene-based nanoplastics using dual flocculants (Ca/Al) and achieved a maximum removal efficiency of 80 % within 6 h under slightly elevated pH conditions. The results revealed that the crystal formation of Al/Ca flocs increased with pH. The same research group further extended their investigations to various combinations of dual flocculants (Mg/Al) and layered double hydroxides (LDH), which are two-dimensional inorganic materials with layered structures (Chen et al., 2021). In that study, polystyrene nanoparticles were used as the target pollutant to understand the role of LDH in removing nanoplastics. In 2023, (Tsai et al., 2023) demonstrated the influence of surface charge and size on the destabilization of nanoplastics using the Fe electrocoagulation process. These authors employed two types of polystyrene nanoparticles prepared through the nanoprecipitation method using sodium dodecyl sulfate (SDS) and cetrimonium bromide solutions (CTAB) to produce negatively-charged SDS-NPs and positively-charged CTAB-NPs. The Fe electrocoagulation process effectively removed 85.3 %, 82.8 %, and 74.7 % of the negatively-charged SDS-NPs with sizes of 90, 200, and 500 nm, respectively.

The current physicochemical methodologies employed for removing nano/microplastics, including adsorption, coagulation/flocculation, flotation, filtration, and magnetic separation, have been found to possess certain limitations, rendering them less desirable in practice. The adsorption method demands the extensive use of chemicals in synthesizing adsorbents, giving rise to apprehensions regarding the associated costs and environmental ramifications. Furthermore, its efficiency is confined to specific target pollutants, and its implementation bears a significant cost burden, necessitating rigorous optimization exercises to attain favorable outcomes (Batool and Valiyaveettil, 2021; Xiong et al., 2020). Analogous challenges emerge from the coagulation/flocculation process that requires high consumption of coagulants/flocculants, raising concerns over cost and environmental implications. Additionally, generating voluminous sludge residues at the bottom of the treatment system introduces complexities in management and disposal, thereby introducing intricacies to the treatment scheme (Lapointe et al., 2020; Shen et al., 2021). As far as the flotation technique is concerned, the dependency on chemical reagents and high equipment costs are valid concerns. Additionally, its sensitivity to aquatic properties may impact its performance in diverse water environments, requiring careful adaptation during application (Wang et al., 2021; Zhang et al., 2021). Moreover, the filtration process shows limited effectiveness in separating nanoparticles (NPs) due to the high cost associated with membranes, and membrane fouling are significant drawbacks to be addressed to optimize its efficiency (Mohana et al., 2021). The magnetic separation of the nanoplastics faces hurdles such as the high consumption of magnetic carrier media, leading to increased costs, and the separation of plastics and magnetic carrier media, necessitating additional processing steps (Shi et al., 2022).

To this end, the efficient removal of nanoplastics prepared using nanoprecipitation, particularly from the source of expanded polystyrene waste (EPS), is emphasized. The reason to choose a pollutant of this kind is to provide baseline information about removing wastes generated through the mechanical breakdown of daily-use polystyrene products or fragmentation of expanded polystyrene foam exposed to sunlight. It is a lesser-known fact that the continuous breakdown of large plastic pieces and microplastics eventually leads to the formation of nanoplastics. According to the work of (Ekvall et al., 2019), the breakdown using a food processor results in the formation of nano-sized polystyrene particles with different shapes and negative surface charges. In addition to the mechanical breakdown, per the study performed by (Song et al., 2020), the direct exposure of EPS to sunlight also causes the fragmentation of microplastics into nanoplastics. For instance, the fragmentation process takes only one month to reduce 5 % of the wt. of the EPS box by photo-degradation. Thus, $\approx 6.7 \times 10^7$ micro and nanoparticles/cm^2 could be generated in countries at a latitude of 34°N. The United States of America generated ≈ 2 million tonnes of polystyrene waste in 2012, of which only 0.9 % was retrieved through recycling. These facts imply that nanoplastics have already been produced from these tons of EPS accumulated over the years. Most of the studies concerning polystyrene-based nanoplastics have been performed using commercially manufactured or nanoparticles synthesized in-house, though the approach fails to emulate real-time situations.

In this work, we demonstrate the conversion of thermocol sheets into polystyrene nanoparticles and their subsequent removal as nanoplastic contaminants in aqueous systems using the electrolysis technique. Unlike previous studies, we simulate real-time situations by avoiding the use of surface-active compounds such as sodium dodecyl sulfate (SDS) and cetrimonium bromide (CTAB). The electrolysis process, which involves particle destabilization and agglomeration through the application of an electrical potential, shows great promise as a green and clean technique for nanoplastic

removal. We specifically employ an electrolysis-assisted flotation (EF) method, where bubbles formed on the electrodes collide with the nanoplastics, bringing them to the surface for removal.

To achieve efficient nanoplastic removal, we optimize various process parameters, including electrode spacing, electrolyte concentration, and nanoplastics concentration. The results demonstrate a high removal efficiency of 95.4 % using the proposed EF method. Notably, the accumulated nanoplastics form a dense and transparent foam-like layer at the top, allowing for easy removal. This creaming process, facilitated by the action of bubbles and coagulants such as Al^{3+} released by the electrodes, presents a novel approach for the separation and removal of nanoplastics. To the best of our knowledge, there are limited studies on the removal of polystyrene-type nanoplastics using electrolysis-based techniques. Moreover, the electrolysis-assisted technique, recognized as a renowned process for separating contaminants from wastewater, offers several benefits, including decreased energy consumption, reduced sludge generation, and minimal environmental repercussions (Perren et al., 2018; Zeboudji et al., 2013). This study provides valuable insights into the removal of nanoplastics from wastewater using the electrolysis-assisted method and offers an alternative approach to address the growing concern of nanoplastic contamination. The findings presented here contribute to the development of sustainable and effective strategies for wastewater treatment and environmental protection.

The remainder of the paper is structured as follows: We first present the nanoprecipitation method to obtain the polystyrene-type nanoplastics from the EPS. Subsequently, the removal of nanoplastics using EF is demonstrated; various factors influencing the efficiency, such as electrode spacing, electrolyte concentration, and nanoplastics concentration, are discussed in detail. Finally, an insight into the stability of the nanoplastics accumulated at the top is provided before presenting the concluding remarks.

2. Materials and methods

2.1. Materials

The expanded polystyrene (EPS) has been sourced from the remnants of the packaging materials. The analytical grade acetone, used as the solvent to initiate precipitation, was procured from Rankem, India. Further, uniform nanoplastic particles were synthesized, and their removal rate was measured using a turbidity meter. We used the aluminium (Al) electrodes as an anode and cathode during the electrolysis process. To demonstrate the elimination of nanoplastics under salt conditions, we prepared an aqueous electrolyte solution using analytical-grade monovalent salt (NaCl) from Sigma-Aldrich, India. The deionized water (18.2 MΩ) from the water purification system procured from Thermo Fisher Scientific India Pvt. Ltd (Smart2Pure^{TM}) was used for all aqueous-based investigations.

2.2. Synthesis of PS particles from waste thermocol sheets

To synthesize EPS particles using the nanoprecipitation technique, we followed the method described by (Rajeev et al., 2016). Firstly, packaging-grade thermocol was cut into smaller pieces and placed in a hot air oven at 160°C for 12 h to remove volatile matter. This process caused the thermocol pieces to shrink, as depicted in Fig. 1, illustrating the step-by-step process of the nanoprecipitation technique followed to precipitate PS nanoparticles. Subsequently, we dissolved the dried samples in acetone at a 1:20 (EPS: acetone) ratio by mass and stirred the mixture using a magnetic stirrer at 500 rpm for 6 h. We allowed impurities to settle and separated the clear solution into a container. For nanoparticle synthesis, 1 mL of EPS solution made of acetone was continuously poured using a burette into a beaker containing 20 mL of deionized water. The drop-wise addition of solution was done at a flow rate of 0.5 mL/minute under constant stirring at a speed of 200 rpm and at room temperature. As a result, water present in the beaker instantly becomes turbid, signifying the precipitation of PS nanoparticles. The suspension containing acetone and EPS was kept initially at 25°C for 8 h and then at 60°C for 4 h to evaporate the acetone and excess solvent. Note: We have given sufficient time for precipitation before heating the mixture to 60°C for 4 h to achieve uniform distribution. Subsequently, we characterized the particles using several characterization techniques. The as-synthesized EPS particles' average diameter and zeta potential measured using dynamic light scattering and electrophoretic light scattering were 175.6 ± 0.83 nm and –39 ± 0.4 mV, respectively.

2.3. Synthetic wastewater

Synthetic wastewater was created to emulate the conditions of industrial wastewater while conducting the treatment with complete control over different parameters. In this study, we studied four parameters affecting wastewater properties. They include turbidity, salt conditions, nanoplastics concentration, and water pH.

The synthetic wastewater was prepared using an aqueous electrolyte solution of known concentration ranging from 10 to 50 mM. The nanoparticles obtained from EPS waste at different concentrations were prepared to make a final total suspended solids (TSS) of 100, 350, and 500 ppm with deionized water to simulate the conditions closer to nanoplastics.

2.4. Industrial wastewater

To demonstrate a proof-of-concept, we performed the electrolysis-assisted removal process on industrial wastewater containing various types of pollutants: Ca and Mg-based salts. This contaminated water was sourced from the process line connected to the inlet of the RO plant. The conductivity, TDS, and pH of wastewater found were 7.2 mS/cm, 5000 ppm, and 7.5, respectively.

In order to simulate the conditions closer to nanoplastics, the nanoparticles obtained from EPS waste at different concentrations were prepared to make a final total suspended solids (TSS) of 100, 350, and 500 ppm with industrial wastewater. Please note that no salts were added in this case, as enough ions were already present as impurities due to various downstream and upstream processes.

2.5. Electrolysis-assisted flotation

The experiments used synthetic wastewater (100 mL) and nanoplastics of size 175.6 ± 0.83 nm. The concentration of nanoplastics used in suspension was 0.35 $mg.mL^{-1}$. The concentration range chosen agrees with several studies reported in literature (Perren et al., 2018; Shen et al., 2022). The studies were carried out in a batch reactor with aluminium electrodes, in parallel combination, with a continuous

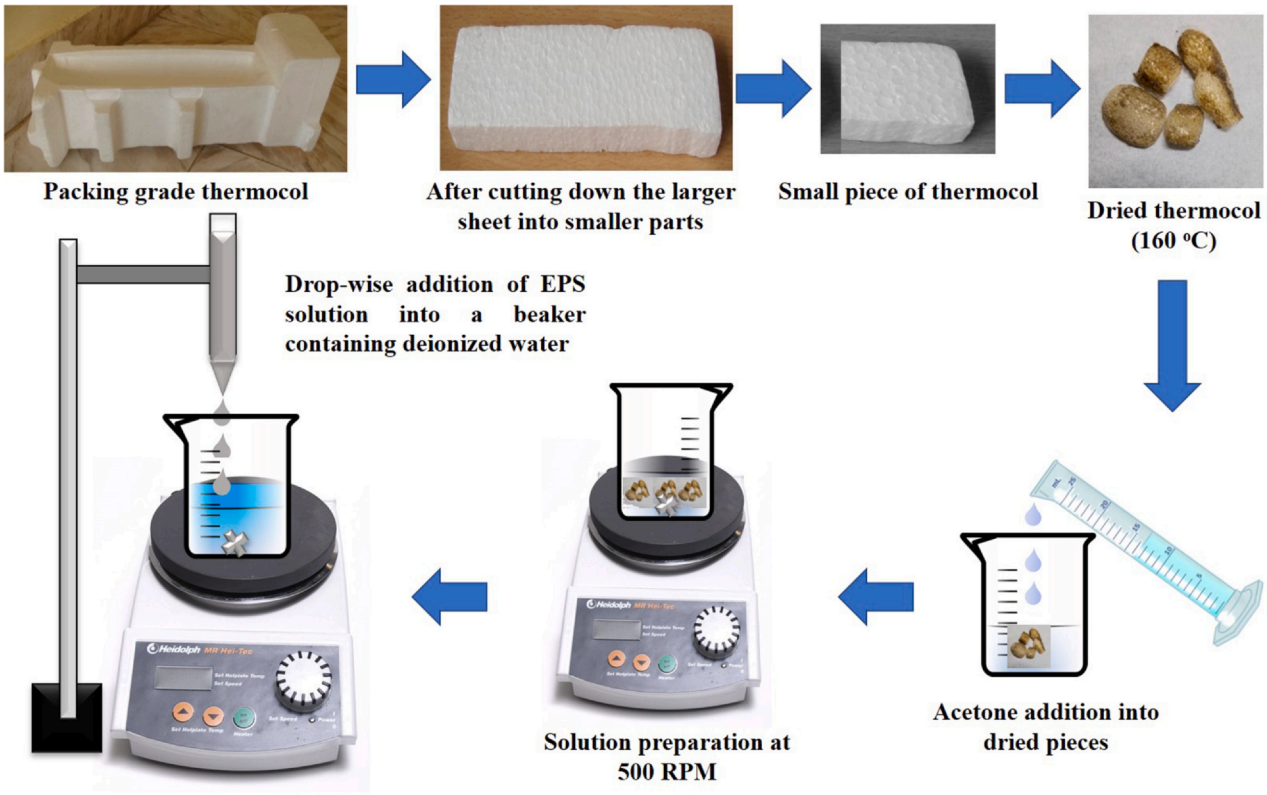

Fig. 1 – Schematic representation depicting the process of nanoparticle synthesis using EPS waste.

stirring speed of 150 rpm (Shen et al., 2022). We have used Keithley's (triple channel) DC power supply to apply the appropriate voltage, as shown in Fig. 2A. The effects of the various experimental parameters, such as electrode spacing, salt (NaCl) concentration and applied voltage on removal efficiency were examined. During this process, two aluminium electrodes of dimensions of 90 mm × 12 mm × 2 mm each were used with an electrode spacing of 1 cm and 2 cm. The concentration of NaCl was varied (i.e. 10, 30 and 50 mM) to investigate the influence of varying current intensities on the removal of nanoplastics. The effect of applied voltage density on nanoplastics removal was studied under 5 V, 10 V and 15 V scenarios at a constant pH of 7.2. For each experiment, the electrochemical set-up was run for 3, 5, 10, 15, and 20 min before switching off. The contaminants were allowed to get close to the interface and stay on top for up to 5 min. Subsequently, the nanoplastics generated near the interface turn turbid or foamy, leaving the solution clear.

Further, the EF process was investigated under light microscopy to understand the structural integrity of the flocs network formed by the nanoplastics and bubbles. For this study, we created the electrolysis setup in a compact petri dish (Diameter: 50 mm) by placing the aluminum electrodes of a specific dimension of 30 mm in length, 12 mm in width, and 2 mm in thickness. These electrodes were positioned at a fixed distance of 2 cm from each other and were connected to a direct current (DC) power supply. Subsequently, the entire setup was carefully positioned onto the microscope stage for analysis using brightfield mode.

2.6. *Removal efficiency measurement*

We have used the turbidity-based technique to quantify the removal of nanoplastics from synthetic wastewater. Turbidity measures the degree of suspended particles in water and is typically measured in NTU (Nephelometric Turbidity Units). It is an essential parameter in water quality monitoring as it can indicate the presence of pollutants and other contaminants (Gregory, 1998). Turbidity has been employed recently in several studies with good selectivity and found to be an effective technique for quantifying nanoparticles (Wyatt, 2018). Turbidity measurement was used by (Arenas et al., 2021) to calculate the removal efficiency of nanoplastics by granular activated carbon (GAC) in a complex matrix. They concluded that it is a valuable and efficient method for determining nanoplastic concentrations in wastewater. In this work, we have used the same approach to determine the removal efficiency of nanoplastics before and after the electrolysis process.

The turbidity of nanoplastics as a function of the concentration was assessed using a turbidity meter and is a measure of decrement in the intensity of incident light due to light scattering of particle suspensions. The greater the concentration of nanoparticles in the suspension, the greater will be the turbidity units. Thus, the turbidity (τ) of colloidal suspension is proportional to the number concentration of nanoparticles as described by the equation below (Shang and Gao, 2014), i.e., Eq. (1).

$$\tau = \frac{1}{4}\pi K d^2 C \tag{1}$$

Where K, d, and C refer to the scattering coefficient, diameter, and concentration of the particles, respectively. Since K and d are constants for the samples involving unique types and uniform sizes of the nanoplastics, the removal efficiency of nanoplastics (R%) for each experiment can be measured using Eq. (2) below.

$$R\% = \frac{\tau_i - \tau_f}{\tau_i} \times 100 \tag{2}$$

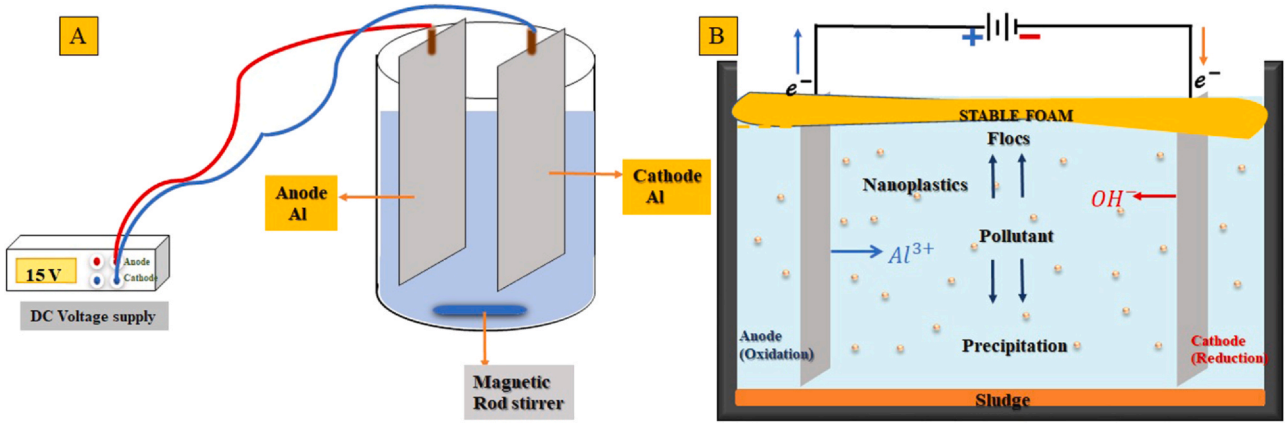

Fig. 2 – Schematic illustration showing (a) experimental setup (b) Mechanism of nanoplastics removal using EF process.

Where τ_i and τ_f represent the initial and final turbidity of the wastewater before and after the electrolysis process, respectively.

A separate set of experiments were conducted using dynamic light scattering (DLS) to complement the results of NTU measurements obtained from a turbidity meter. DLS measures the photon count rate, an indicator of the nanoplastics concentration. That is, the scattered light intensity (I) is proportional to the photon count rate (P) of colloidal dispersions as described by Eq. (3) below (Liu et al., 2008; Vysotskii et al., 2009).

$$I = BP \tag{3}$$

In the above equation, B refers to a constant.

Assuming that the size (d) of nanoplastics is smaller than the wavelength of the incident light, Rayleigh scattering may be applied to relate the scattered light intensity and concentration of nanoplastics (C) as shown below in Eq. (4) (Shang and Gao, 2014).

$$I = I_0 \alpha \left(\frac{m^2 - 1}{m^2 + 1} \right)^2 d^6 C \tag{4}$$

Wherein I_0 is the incident light intensity, α is an instrument coefficient, which is a function of scattering angle (θ), the distance between the point of observation and the particle (R), and the wavelength of the incident light (λ), and m is defined as the refractive index of the medium.

If a known concentration of the colloidal sample (C_1) is available, a linear combination of concentration of nanoplastics (C_2) and derived count rate (P) can be established as described below by Eq. (5).

$$C_2 = \frac{P_2}{P_1} C_1 \tag{5}$$

Alternatively, the % removal efficiency can also be calculated using the following equation:

$$R\% = \frac{P_i - P_f}{P_i} \times 100 \tag{6}$$

Please note that we ensured the consistency of the attenuation factor while obtaining the derived count rate. The derived count rate is the reported count rate divided by the attenuation factor.

2.7. *Characterization*

The as-synthesized nanoplastics were analyzed using field emission scanning electron microscopy (FESEM), Make: JEOL Ltd., Japan and Model: JSM-7610F, to characterize the particle morphology and deduce the average size. The hydrodynamic radius of EPS particles was determined using the dynamic light scattering (DLS), Make: Malvern Instruments and Model: Zetasizer Nano ZSP. The zeta potential of EPS was measured based on the electrophoretic light scattering (ELS) study using Zetasizer procured from Malvern Instruments, Model: Zetasizer Nano ZSP. The turbidity meter (Make: OAKTON, Model: T100) and DLS were employed to obtain nephelometric turbidity units (NTU) and photon count rate, respectively, as a function of the time of electrolysis-assisted flotation to investigate the creaming process. Fourier-transform Infrared spectroscopy (Make: Thermo Scientific Nicolet, Model: iS50) was used to identify the chemical composition of EPS particles. Thermal gravimetric analysis (TGA), make: TA instrument, model: SDT650, was carried out to capture the decomposition profiles of the EPS particles. The inverted microscopy (Make: Carl Zeiss; Model: AxioVert.A1) was used to visualize the phenomenon of electrolysis assisted flotation process. The scanning electron microscopy (SEM), JEOL, JSM-6610, was utilized to examine the structural aspects of flocs produced by the electrolysis-assisted flotation method.

3. Results and discussion

First, we discuss the characteristic features of EPS particles inferred from various characterization techniques. Fig. 3A depicts the representative scanning electron microscopic image corresponding to the EPS surface morphology. The particles obtained are spherical and slightly poly-dispersed. Fig. 3B depicts the size distribution of nanoplastics obtained by performing image analysis using ImageJ software. Based on 250 representative particles, the average size is 148 ± 22 nm. The close examination of the several reported data from the literature indicates that the deviation of 15–20 % is quite typical in synthesizing polystyrene (PS) nanoparticles from the EPS waste (Rajeev et al., 2016). Nevertheless, such variation is not detrimental to our studies considering the polydispersity associated with the microplastics and nanoplastics distribution in real-time application.

Fig. 4 displays the FTIR spectrum of as-synthesized EPS nanoparticles. The spectra observed between 3060 and 2853 cm^{-1} correspond to the characteristic bands for aromatic and aliphatic C–H stretching, while the peak at 1598 cm^{-1} reiterates the presence of aromatic stretch, i.e., C = C. On the other hand, the peak at 3443 cm^{-1} indicates the existence of OH

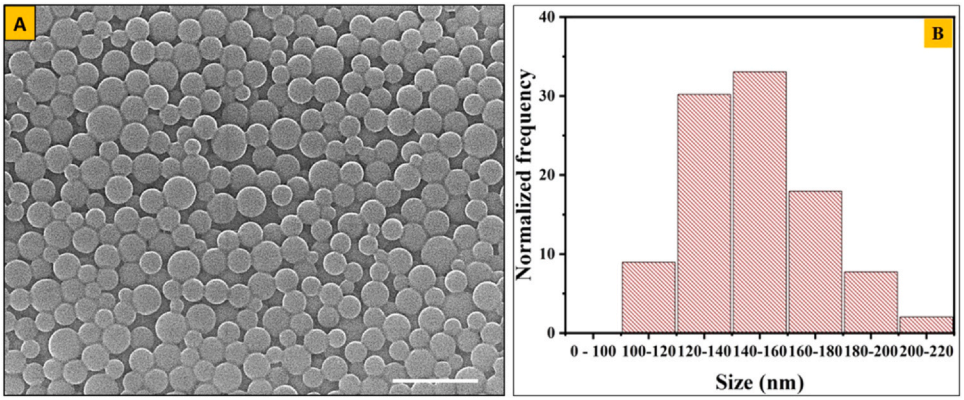

Fig. 3 – Structural characterization of EPS particles. A) FESEM image, B) size distribution obtained by analyzing the FESEM images using ImageJ. The scale bar given in the image corresponds to 500 nm.

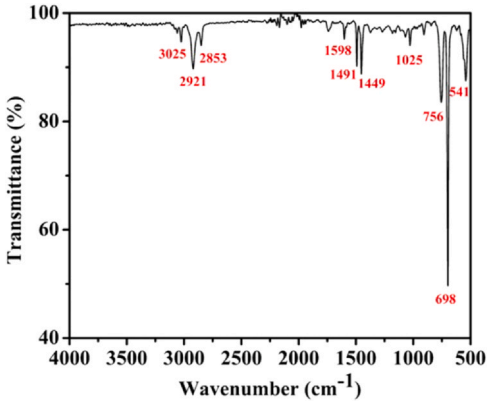

Fig. 4 – FTIR spectra of polystyrene nanoparticles made from EPS waste using the nanoprecipitation method.

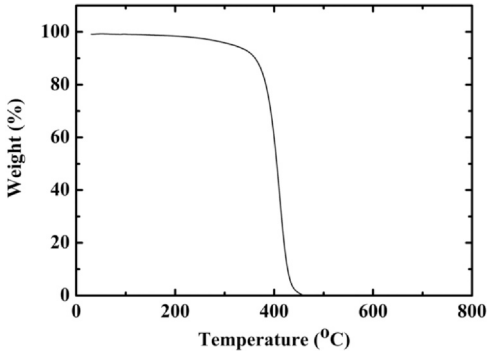

Fig. 5 – Thermal gravimetric analysis (TGA) of polystyrene nanoparticles obtained from EPS waste.

stretching. In short, the appearance of characteristic peaks at three different regions, 1) 400–900 cm^{-1}, 2) 900–2000 cm^{-1}, and 3) 2800–3200 cm^{-1}, reaffirm its existence identical to that of the chemical composition of PS. Further, the characteristics of polystyrene observed by us are in good agreement with the FTIR spectrum reported by Rajeev et al. (2016).

Fig. 5 displays the thermal decomposition profile of polystyrene nanoparticles obtained from EPS waste. The respective polystyrene sample was subjected to temperature sweep from 30°C to 800°C with a heating rate of 10°C/min. The decomposition data vis-a-vis temperature was in good agreement with the reported values of polystyrene, i.e., initial decomposition temperature = 300°C and corresponding half decomposition temperature = 364°C (Rajeev et al., 2016).

Thus, combining various characterization techniques discussed so far establishes the physicochemical properties close to that of pure polystyrene materials. Therefore, the as-synthesized nanoparticles can be treated similarly to the nanoplastics, which is paramount in pursuing the electrolysis-based wastewater treatment containing plastic particles. The basis for choosing negatively charged polystyrene instead of positively charged one is that almost 93 % of micro or nanoplastics waste collected from various channels are polyethene/polyethylene derived compounds, which are negatively charged (Gouin et al., 2015). Hence, to simulate similar conditions, we pursued our study using the negatively charged polystyrene particles less than 1μm by recovering them from the EPS waste.

Before heading the topic into removing nanoplastics, we discuss the underlying principles of the proposed method induced by electrolysis. In this process, coagulants are generated in situ due to the oxidation of the metal anode when an electric current is passed through it (Pulkka et al., 2014) At the anode, Al^{3+} ions are liberated and dissolved in the suspension. The dissolved metal ions combine with hydroxyl ions in the water to form metal hydroxides acting as coagulants (Behbahani et al., 2011). These coagulants neutralize the surface charges of pollutants/nanoplastics, moving particles closer to each other due to the decrease in the electrostatic force of repulsion. The $Al(OH)_3$ produced by anodic Al dissolution is believed to be more effective at coagulating pollutants in wastewater. However, the passivation of Al anodes and the impermeable film formed on cathodes can hinder the performance of electrocoagulation (Holt et al., 2005). Following reactions occur at the anode and cathode (Perren et al., 2018; Shen et al., 2022).

At Anode:

$$Al_{(s)} \longrightarrow Al^{3+}_{(aq)} + 3e^- \quad (7)$$

$$2H_2O_{(l)} \longrightarrow 4H^+_{(aq)} + O_{2_{(g)}} + 4e^- \quad (8)$$

At Cathode:

$$Al^{3+}_{(aq)} + 3e^- \longrightarrow Al_{(s)} \quad (9)$$

$$2H_2O_{(l)} + 2e^- \longrightarrow H_{2(g)} + 2OH^- \quad (10)$$

$$Al^{3+}_{(aq)} + 3OH^- \longrightarrow Al(OH)_{3(s)} \quad (11)$$

The bubbles of hydrogen and oxygen generated during the electrolysis of water move upwards in the liquid and lead to the effective removal of contaminants (Linares-Hernández

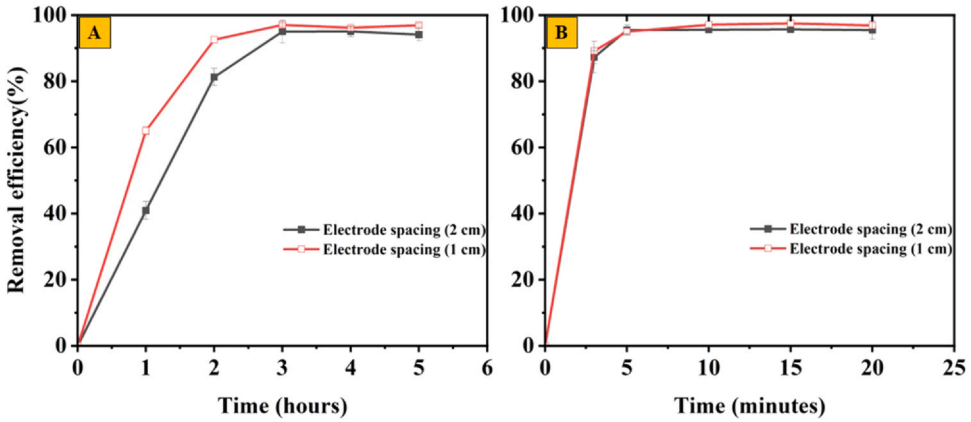

Fig. 6 – (A) Effect of electrode spacing on the removal of nanoplastics from wastewater in the EF process in the absence of electrolyte. (B) Effect of electrode spacing with electrolyte (NaCl) on the removal of nanoplastics from wastewater using EF process.

et al., 2009; Arroyo et al., 2009; El-Naas et al., 2009). We believe the generated metal ions combine with the nanoplastics present in the water, which gets removed via the formation of foam collected on the top of the reactor. This foam formation depends on several factors, such as hydrogen and oxygen gas bubble formation, type of contaminant, surface tension, zeta potential, temperature, and pH of the system for effective interaction of the gas bubbles and particles in the wastewater (Sillanpää and Shestakova, 2017). From the Eqs. (8) and (10) mentioned above, the liberation of oxygen (O_2) and hydrogen (H_2) gas takes place at the anode and cathode, respectively, that forms gas bubbles (please refer to Fig. 2B). As they rise, these gas bubbles will entrap many organic compounds and pollutants in the wastewater. All these particles entrapped in the gas bubbles rise and get collected near the interface, causing foam formation, which may be skimmed off later to remove these compounds from the water.

To this end, we show the removal of as-synthesized nanoplastics using the EF process, wherein treatment of these nanoplastics was dependent on various operating parameters such as inter-electrode distance, applied voltage, and electrolyte concentration. We investigated the effect of these parameters to improve the removal rate of nanoplastics from wastewater. We also demonstrate the formed foam's stability after removing pollutants. However, we initially examined the pollutant's removal and settling without EF through control studies. We observed the evidence of the removal of particles in the presence of electrolytes due to charge neutralization and accumulation of nanoplastics. On the other hand, no significant particle removal was observed in the absence of electrolytes. The removal efficiency in the absence of electrolytes was only 1.25 %, while it was 99.6 % in the presence of electrolytes after 27 days.

3.1. *Effect of electrode spacing*

To understand the effect of electrode spacing, we have varied the distance between the aluminium electrodes from 1 cm to 2 cm while keeping other parameters constant. According to many investigations, inter-electrode spacing has been essential in electrolysis. According to Bukhari (2008), increasing the distance between the electrodes may decrease its efficiency and hence can increase the capital cost for removing total suspended solids (TSS) from municipal waste. The investigations conducted by Attour et al. (2014) and Merzouk et al. (2010) have also indicated that when the gap between the electrodes is widened, the electrical conductivity of the solution decreases. As a result, the resistivity of the solution increases, leading to reduced metal dissolution. This reduction in metal dissolution contributes to decreased overall removal efficiency.

The effect of electrode spacing on the removal efficiency is shown in Fig. 6A. The experiments corresponding to the one shown in Fig. 6A were performed without electrolytes. The other experimental conditions are as follows: Concentration of nanoplastics –0.35 $mg.mL^{-1}$, inter-electrode distance –1 & 2 cm, stirring speed –150 rpm, applied voltage –15 V, pH of the solution –7.2. The removal rate found were 65.7 %, 91.5 %, 93 %, 95.1 %, 93.7 % at 1 cm and 40.8 %, 80.1 %, 91.2 %, 93.3 %, 92.2 % at 2 cm inter-electrode distance after 1, 2, 3, 4 and 5 h of EF process, respectively, with electrodes being aluminium. However, the removal of nanoplastics was significantly improved in the initial 3 h by decreasing the electrode spacing from 2 cm to 1 cm. This enhanced performance can be attributed to the electrostatic effects, which could cause higher movement of ions, leading to a high creaming rate (Khandegar and Saroha, 2014).

The impact of nanoplastic removal was studied with varying inter-electrode distances at a fixed electrolyte (NaCl) concentration of 50 mM. As shown in Fig. 6B, the removal rate of nanoplastics was greatly affected by the addition of electrolytes as it reduced the removal rate from 3 h to 5 min. Although varying the distance between the electrodes did not show any significant effect in the presence of an electrolyte, it showed a slight increment in the removal efficiency of nanoplastics when the electrode distance was reduced from 2 cm to 1 cm. Other operating parameters are as follows: Concentration of nanoplastics –0.35 $mg.mL^{-1}$, pH of the solution –7.2, electrolyte concentration –50 mM, stirring speed –150 rpm, and the applied voltage –15 V. The removal efficiency of nanoplastics achieved was 87.2 %, 95.4 %, 95.5 %, 95.6 %, 93.33 % and 89.1 %, 94.9 %, 97.1 %, 97.4 %, 96.8 % at 2 cm and 1 cm electrode spacing after 3, 5, 10, 15, and 20 min of EF process, respectively. Adding electrolytes to the solution increases the dissolution of Al^{3+} ions. Consequently, significant screening of nanoplastics' charge was achieved primarily due to these ions (Shen et al., 2022).

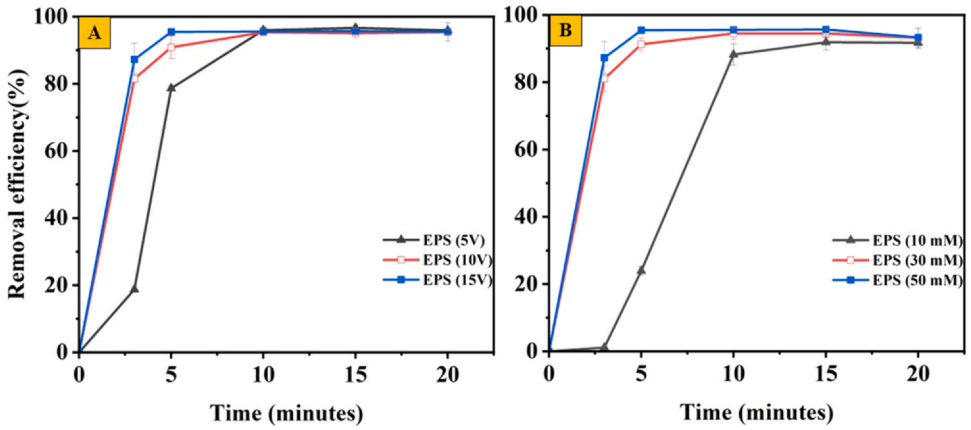

Fig. 7 – (A) Effect of applied voltage on the removal of nanoplastics from wastewater using EF process. (B) Effect of electrolyte concentration (NaCl) on the removal of nanoplastics from wastewater using EF process.

3.2. *Effect of applied voltage*

The effect of voltage on the EF process is paramount to improving the reaction rate of the process. According to Faraday's law, the dissolution of Al^{3+} ions increases when the amount of current that passes through the Al anode increases. These Al^{3+} ions dissolve into the solution and combine with the OH^- present in water to form the aluminium hydroxide, which helps in increasing the removal efficiency of the nanoplastics (Shen et al., 2022). Further, the increased applied voltage also increases the number density of hydrogen bubbles produced at the cathode. These hydrogen bubbles enhance the mixing phenomena of aluminium hydroxides with nanoplastics and improve the flotation of nanoplastics, which increases the removal efficiency (Guo et al., 2006; El-Ashtoukhy et al., 2013). Furthermore, it was also found that by increasing the applied voltage, the amount of hydrogen bubbles increased, along with a reduction in the size, resulting in faster removal of nanoplastics and sludge flotation (El-Ashtoukhy et al., 2013; Elkhatib et al., 2021; Akarsu et al., 2021).

The effect of applied voltage density on nanoplastic removal was performed under 5 V, 10 V and 15 V, respectively, while keeping the other operating parameters constant. Fig. 7A shows the removal rate of nanoplastic over time under different applied voltage densities in the EF process. The removal efficiency was observed at 18.7 %, 78.6 %, 95.9 %, 96.6 %, 95.8 % at 5 V, 81.5 %, 90.15 %, 84.6 %, 82.1 %, 77.0 % at 10 V and 87.2 %, 95.4 %, 95.5 %, 95.6 %, 93.3 % at 15 V, respectively, after 3, 5, 10, 15, 20 min of the EF process.

3.3. *Effect of electrolyte concentrations*

We have examined the effects of electrolyte concentration (NaCl) based on synthetic wastewater treatment. The electrolyte is a crucial parameter that reduces the reaction time and affects the operating cost and electricity consumption. The removal efficiency of nanoplastics was thoroughly investigated by varying the salt concentrations (NaCl) from 10 mM to 50 mM, as shown in Fig. 7B. Adding electrolytes to the solution would increase the conductivity of the solution, thereby increasing the removal efficiency of microplastics (Shen et al., 2022; Perren et al., 2018). Shalaby et al. (2014) demonstrated that the formation of $Al(OH)_3$ in the solution could be increased by adding the electrolytes. As a result, the process led to enhanced phosphorus removal efficiency. Our results show that the removal efficiency of nanoplastics was increased with an increase in electrolyte concentration from 10 mM to 50 mM with aluminium electrodes. We kept other parameters constant; concentration of nanoplastics –0.35 $mg.mL^{-1}$, electrode spacing –2 cm, pH of the solution –7.2, stirring speed –150 rpm, and applied voltage –15 V. The removal efficiency of nanoplastics achieved at different salt concentrations was 1.11 %, 23.9 %, 88.2 %, 91.8 %, 91.7 % at 10 mM, 81.0 %, 91.2 %, 94.5 %, 94.5, 93.1 % at 30 mM and 87.2 %, 95.4 %, 95.5 %, 95.6 %, 93.33 % at 50 mM after 3, 5, 10, 15, and 20 min of the EF process, respectively.

3.4. *Effect of nanoplastics concentration*

This section discusses a straightforward DLS-based approach used to complement the turbidity measurements. The derived count rate obtained as a function of the EF time recapitulates the findings established by the turbidity studies. Fig. 8A refers to the removal efficiency data obtained with the help of DLS and turbidity meter. The maximum removal efficiency obtained using the DLS and turbidity meter is 94 % and 95 %, respectively, making the EF process more enticing. Further, the synthetic water with different nanoplastics concentrations was exposed to EF treatment to understand the role of nanoplastics loading. For studies on various nanoplastics concentrations, the derived count rate obtained from DLS has been used to deduce the removal efficiency. Fig. 8B displays the performance of the EF process in treating the synthetic wastewater containing nanoplastics of varying concentrations ranging from 0.1 to 0.5 $mg.mL^{-1}$ or 100–500 ppm. As depicted by Fig. 8, the maximum removal efficiency found is almost the same irrespective of the concentration employed, which is in favor of the reported work by Elkhatib et al. (2021). However, the EF process for the extended period of 10 min ensures that sufficient coagulants are generated in the dispersions to neutralize the charge of the nanoplastics. Thus, the maximum removal efficiency of 0.5 $mg.mL^{-1}$ corresponding to 10 min EF is 96.7 %.

While the swift change in the removal rate could be attributed to the rapid generation of bubbles and its intense action in drifting the nanoplastics away from the bulk, the reason for a slight dip in the efficiency after maxima are linked to poor-moderate strength of flocs and breakdown of films at a later stage. The direct visualization of the EF process through a digital camera revealed that the continuous and swift generation of bubbles during the EF process starts

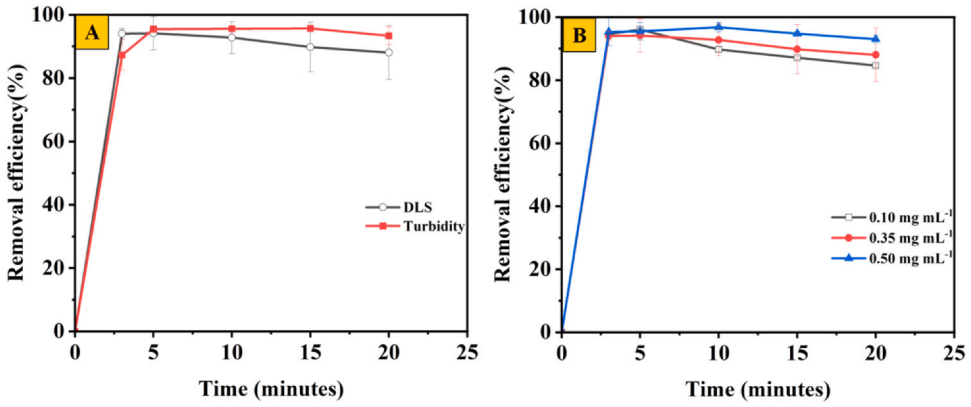

Fig. 8 – (A) DLS-based measurements validating the results of turbidity meter. (B) Removal efficiency as a function of time for different nanoplastics concentrations.

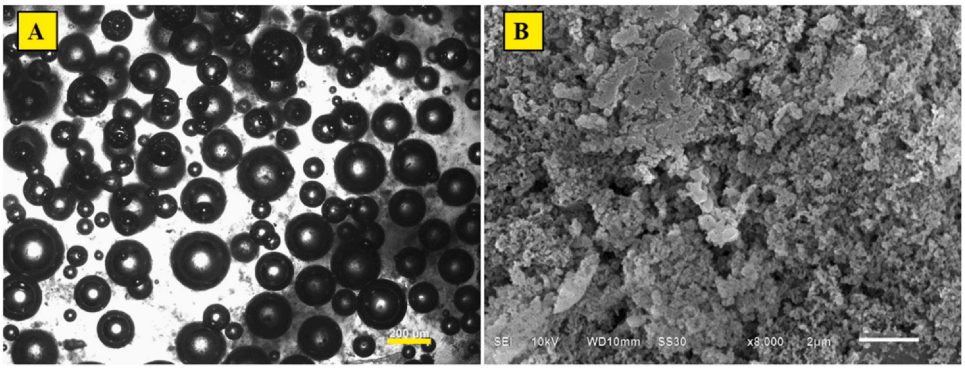

Fig. 9 – The representative light microscopic image showing the structure of bubbles formed at the interface at the coalescence/flocs state (A) and the SEM image capturing the state of nanoplastics collected from the top (B).

drifting the aggregates/flocs of nanoplastics away from the bulk as soon as they collide. The video demonstrating the mass movement of aggregates/flocs nanoplastics under the influence of bubbles is provided in the supplementary information (SI). Please refer to Video 1 provided in the SI for the details. This observation can be strengthened further by visualizing the phenomenon under an inverted light microscope and capturing the structure of flocs. It can be noted that the details of the experiments related to the light microscope are given in section 2.5. We understand that the sudden fall in the efficiency is more prominent in the case of 0.1 mg/mL concentration of nanoplastics than in 0.35 and 0.5 mg/mL. This factor could be explained by the fact that the strength of flocs formed by the nanoplastics of concentration 0.1 mg/mL could be weaker than those of the higher concentration. It can be inferred from Video 2 (Please refer to Video 2 provided in the SI for details) that the flocs formed by the combined action of coalescence of bubbles and nanoplastics get disengaged due to the turbulence caused by incoming bubbles, leading to a slight breakdown of the film after 10 min of EF process. This phenomenon is more prominent in the case of 0.1 mg/mL than 0.35 mg/mL, as demonstrated by Video 2. Subsequently, the breakdown of the film causes a re-entrant of nanoplastics in bulk, ultimately resulting in a slight dip in the removal efficiency in a particular case. Fig. 9A and B display the representative light and electron microscopic images corresponding to the structure of bubbles/flocs formed at the interface and the nanoplastics after removing them by scraping and drying, respectively. Additionally, Fig. 9B demonstrates that removing the nanoplastics from the top is possible by simply collecting the sludge formed at the top, in contrast to the conventional coagulation/flocculation process wherein the sludge forms at the bottom.

Supplementary material related to this article can be found online at doi:10.1016/j.cherd.2023.08.038.

3.5. *Stability of a foamy layer*

In EF, foam stability significantly affects the process's efficiency and hence the treatment's effectiveness. Foam is generated during EF due to the production of hydrogen and oxygen gases as bubbles at the electrodes. While these gas bubbles rise, they interact with the pollutants, driving them to the interface's vicinity. The collection of all nanoplastics generates a foamy layer-like appearance at the top.

Here, we denote the foam stability in terms of the removal efficiency of nanoplastics by measuring the turbidity of the apparent phase at the bottom of the reactor. The idea is to monitor the NTU of bulk solution as a function of time to evaluate the net removal efficiency. If foam destabilizes over time, the nanoplastics trapped within the turbid phase will eventually diffuse back to the bulk. This phenomenon reverses the direction of the flow of the nanoparticles and thereby increases the turbidity in bulk. For deducing the net removal efficiency of the nanoplastics, we observed foam stability after running the reactor for 5 min at the optimized parameters. Note: We chose 5 min as a reference point as we observed the maximum efficiency within this time scale. After 5 min of operation, solid foam appeared on top of the container and turbidity of the apparent phase was measured. We noticed that the foam stability decreased from 5 min to

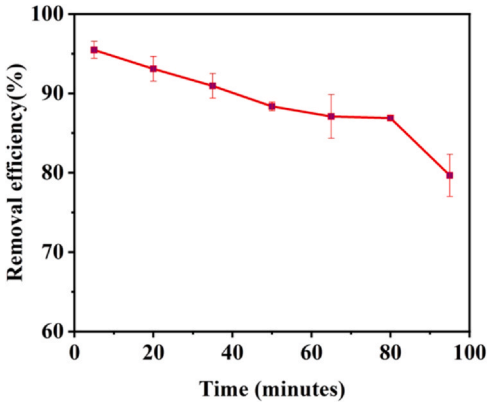

Fig. 10 – Stability analysis of the generated foam as a function of time.

95 min. Therefore we conclude that the turbidity of the solution induced by destabilization increases with time due to gravitational force, as shown in Fig. 2B.

The removal efficiency of nanoplastics observed was 95.4 %, 93 %, 90.9 %, 88.3 %, 87.0 %, 86.8 %, and 79.6 % after 5, 20, 35, 50, 65, 80, and 95 min, respectively, when the reactor was switched off after 5 min of EF process. As the foam got destabilized, the turbidity of the clear phase increased, and the removal efficiency decreased over time (please refer to Fig. 10). We observed that the stability of the foam decreased from 5 min to 95 min, with a maximal stability and removal efficiency of 95.45 % at 5 min and a minimum of 79.65 % at 95 min, indicating significant destabilization of the foam. Additionally, as time progressed, the foam became destabilized, and the clear phase became turbid, indicating that the solution was contaminated with the resuspension of pollutants in the synthetic water. It comes to say that it is essential to complete the required scraping operation within a particular duration to ensure maximum separation. For instance, one must perform necessary actions within 20 min to eliminate 93 % of pollutants or within 35 min to achieve 91 % removal of nanoplastics (pollutants). Therefore, the given stability data may be referred to as baseline information before performing a cleanup on a large scale.

3.6. *Proof-of-concept*

This section discusses the proof-of-concept (POC) for removing nanoplastics via an industrial wastewater-based EF process. As mentioned in the experimental section, industrial wastewater containing pre-loaded nanoplastics was treated without adding salts. The initial dispersions subjected to treatment had conductivity values of 7.2 mS/cm, which indicated that the electrolyte strength was sufficient to promote coagulation. The video showing the start-to-finish EF process is provided in the supplementary section. It is clear from the video (Please refer to Video 3 given in the SI for details) that after 5 min of EF treatment, the sample's cloudiness turned into a clear solution because the creaming caused the nanoplastics in the dispersion to drift quickly towards the air-water interface. Further, the nanoplastics concentration of treated industrial wastewater was found to be 0.03 $mg.mL^{-1}$ or 30 ppm with the maximum removal efficiency of 91.4 %. This demonstration provides a profound applicability of the method in cleaning industrial wastewater containing nanoplastics. Further, this result could be used as baseline information to extend the concepts to perform a large-scale wastewater cleanup.

4. Conclusion

This work demonstrates the EF process as an effective method for removing nanoplastic waste from synthetic wastewater. The proposed process is an efficient technique with higher removal rates, lower energy consumption and lesser sludge generation with low environmental impact. Since the process yields no secondary wastes, it can be considered a green technique for removing nanoplastics. Further, the maximum removal efficiency of PS-based nanoplastics could be achieved at an electrolyte (NaCl) concentration of 50 mM, pH of the solution of 7.2, electrode spacing of 2 cm and an applied voltage of 15 V. The removal of 95.4 % of pollutants from synthetic wastewater containing nanoplastics at a concentration of 0.35 $mg.mL^{-1}$ or 350 ppm was achieved after 5 min of the EF process. With the maximum removal efficiency of 94.1 %, the derived count rate obtained from DLS complements the turbidity measurements in a significant way. Eliminating nanoplastics using EF is a practical and effective solution for addressing the growing problem of nanoplastics in the environment. Further research is needed to optimize the effectiveness of this process for different types of nanoplastics present in wastewater. However, EF has the potential to play a crucial role in the management and reduction of nanoplastics pollution in the aquatic environment. It may be used as an effective and green method to treat larger volumes of wastewater with higher concentrations of nanoplastics. The research into using an automated dip-coating procedure to remove nanoplastics from the interface is ongoing.

Author contributions

All authors contributed to the study conception and design. Vishal Singh performed material preparation, data collection, and analysis. Vishal Singh wrote the first draft of the manuscript. Chandra Shekhar did the data collection and analysis on dynamic light scattering. Manigandan and Vijay Anand were credited for reviewing and shaping the manuscript. Financial assistance for the research: Vijay Anand.

Funding

Department of Science and Technology, Government of India, for the Technology Innovation Hub at the Indian Institute of Technology Ropar in the framework of the National Mission on Interdisciplinary Cyber-Physical Systems (NM-ICPS).

Data availability

The experimental results used for the analysis will be made available on a reasonable request basis.

Declaration of Competing Interests

The authors declare that they have no known competing financial interests or personal relationships that could have appeared to influence the work reported in this paper.

Acknowledgments

This work was conducted through the support of the Water and Soil Quality Assessment domain, AWaDH, IIT Ropar. The authors acknowledge the grant from the Department of Science and Technology, Government of India, for the Technology Innovation Hub at the Indian Institute of Technology Ropar in the framework of the National Mission on Interdisciplinary Cyber-Physical Systems (NM-ICPS).

Ethics approval

Not applicable.

References

Akarsu, C., Kumbur, H., Kideys, A.E., 2021. Removal of microplastics from wastewater through electrocoagulation-electroflotation and membrane filtration processes. Water Sci. Technol. 84 (7), 1648–1662.

Arenas, L.R., Gentile, S.R., Zimmermann, S., Stoll, S., 2021. Nanoplastics adsorption and removal efficiency by granular activated carbon used in drinking water treatment process. Sci. Total Environ. 791, 148175.

Arroyo, M., Pérez-Herranz, V., Montanes, M., García-Antón, J., Guinon, J., 2009. Effect of ph and chloride concentration on the removal of hexavalent chromium in a batch electrocoagulation reactor. J. Hazard. Mater. 169 (1–3), 1127–1133.

Attour, A., Touati, M., Tlili, M., Amor, M.B., Lapicque, F., Leclerc, J.-P., 2014. Influence of operating parameters on phosphate removal from water by electrocoagulation using aluminum electrodes. Sep. Purif. Technol. 123, 124–129.

Batool, A., Valiyaveettil, S., 2021. Surface functionalized cellulose fibers–a renewable adsorbent for removal of plastic nanoparticles from water. J. Hazard. Mater. 413, 125301.

Behbahani, M., ALAVI, M.M., Arami, M., 2011. A comparison between aluminum and iron electrodes on removal of phosphate from aqueous solutions by electrocoagulation process. Int. J. Environ. Res.

Bianco, A., Sordello, F., Ehn, M., Vione, D., Passananti, M., 2020. Degradation of nanoplastics in the environment: Reactivity and impact on atmospheric and surface waters. Sci. Total Environ. 742, 140413.

Bond, T., Ferrandiz-Mas, V., Felipe-Sotelo, M., Van Sebille, E., 2018. The occurrence and degradation of aquatic plastic litter based on polymer physicochemical properties: a review. Crit. Rev. Environ. Sci. Technol. 48 (7–9), 685–722.

Bukhari, A.A., 2008. Investigation of the electro-coagulation treatment process for the removal of total suspended solids and turbidity from municipal wastewater. Bioresour. Technol. 99 (5), 914–921.

Chen, Z., Liu, J., Chen, C., Huang, Z., 2020. Sedimentation of nanoplastics from water with ca/al dual flocculants: characterization, interface reaction, effects of ph and ion ratios. Chemosphere 252, 126450.

Chen, Z., Huang, Z., Liu, J., Wu, E., Zheng, Q., Cui, L., 2021. Phase transition of mg/al-flocs to mg/al-layered double hydroxides during flocculation and polystyrene nanoplastics removal. J. Hazard. Mater. 406, 124697.

Dawson, A.L., Kawaguchi, S., King, C.K., Townsend, K.A., King, R., Huston, W.M., Bengtson Nash, S.M., 2018. Turning microplastics into nanoplastics through digestive fragmentation by antarctic krill. Nat. Commun. 9 (1), 1–8.

Ekvall, M.T., Lundqvist, M., Kelpsiene, E., Šileikis, E., Gunnarsson, S.B., Cedervall, T., 2019. Nanoplastics formed during the mechanical breakdown of daily-use polystyrene products. Nanoscale Adv. 1 (3), 1055–1061.

El-Ashtoukhy, E., El-Taweel, Y., Abdelwahab, O., Nassef, E., 2013. Treatment of petrochemical wastewater containing phenolic compounds by electrocoagulation using a fixed bed electrochemical reactor. Int. J. Electrochem. Sci. 8 (1), 1534–1550.

Elkhatib, D., Oyanedel-Craver, V., Carissimi, E., 2021. Electrocoagulation applied for the removal of microplastics from wastewater treatment facilities. Sep. Purif. Technol. 276, 118877.

El-Naas, M.H., Al-Zuhair, S., Al-Lobaney, A., Makhlouf, S., 2009. Assessment of electrocoagulation for the treatment of petroleum refinery wastewater. J. Environ. Manag. 91 (1), 180–185.

Erni-Cassola, G., Zadjelovic, V., Gibson, M.I., Christie-Oleza, J.A., 2019. Distribution of plastic polymer types in the marine environment; a meta-analysis. J. Hazard. Mater. 369, 691–698.

Geyer, R., Jambeck, J.R., Law, K.L., 2017. Production, use, and fate of all plastics ever made. Sci. Adv. 3 (7), e1700782.

Gouin, T., Avalos, J., Brunning, I., Brzuska, K., De Graaf, J., Kaumanns, J., Koning, T., Meyberg, M., Rettinger, K., Schlatter, H., et al., 2015. Use of micro-plastic beads in cosmetic products in europe and their estimated emissions to the north sea environment. SOFW J. 141 (4), 40–46.

Gregory, J., 1998. Turbidity and beyond. Filtr. Sep. 35 (1), 63–67.

Guo, Z.-R., Zhang, G., Fang, J., Dou, X., 2006. Enhanced chromium recovery from tanning wastewater. J. Clean. Prod. 14 (1), 75–79.

Holt, P.K., Barton, G.W., Mitchell, C.A., 2005. The future for electrocoagulation as a localised water treatment technology. Chemosphere 59 (3), 355–367.

Khandegar, V., Saroha, A.K., 2014. Electrochemical treatment of textile effluent containing acid red 131 dye. J. Hazard. Toxic. Radioact. Waste 18 (1), 38–44.

Lapointe, M., Farner, J.M., Hernandez, L.M., Tufenkji, N., 2020. Understanding and improving microplastic removal during water treatment: impact of coagulation and flocculation. Environ. Sci. Technol. 54 (14), 8719–8727.

Li, Y., Li, W., Jarvis, P., Zhou, W., Zhang, J., Chen, J., Tan, Q., Tian, Y., 2020. Occurrence, removal and potential threats associated with microplastics in drinking water sources. J. Environ. Chem. Eng. 8 (6), 104527.

Linares-Hernández, I., Barrera-Díaz, C., Roa-Morales, G., Bilyeu, B., Ureña-Núñez, F., 2009. Influence of the anodic material on electrocoagulation performance. Chem. Eng. J. 148 (1), 97–105.

Liu, X., Dai, Q., Austin, L., Coutts, J., Knowles, G., Zou, J., Chen, H., Huo, Q., 2008. A one-step homogeneous immunoassay for cancer biomarker detection using gold nanoparticle probes coupled with dynamic light scattering. J. Am. Chem. Soc. 130 (9), 2780–2782.

Merzouk, B., Madani, K., Sekki, A., 2010. Using electrocoagulation–electroflotation technology to treat synthetic solution and textile wastewater, two case studies. Desalination 250 (2), 573–577.

Mohana, A.A., Farhad, S., Haque, N., Pramanik, B.K., 2021. Understanding the fate of nano-plastics in wastewater treatment plants and their removal using membrane processes. Chemosphere 284, 131430.

Napper, I.E., Thompson, R.C., 2019. Environmental deterioration of biodegradable, oxo-biodegradable, compostable, and conventional plastic carrier bags in the sea, soil, and open-air over a 3-year period. Environ. Sci. Technol. 53 (9), 4775–4783.

Perren, W., Wojtasik, A., Cai, Q., 2018. Removal of microbeads from wastewater using electrocoagulation. ACS Omega 3 (3), 3357–3364.

Picó, Y., Manzoor, I., Soursou, V., Barceló, D., 2022. Microplastics in water, from treatment process to drinking water: analytical methods and potential health effects. Water Emerg. Contam. Nanoplast. 1 (3), 13.

Pulkka, S., Martikainen, M., Bhatnagar, A., Sillanpää, M., 2014. Electrochemical methods for the removal of anionic contaminants from water–a review. Sep. Purif. Technol. 132, 252–271.

Rajeev, A., Erapalapati, V., Madhavan, N., Basavaraj, M.G., 2016. Conversion of expanded polystyrene waste to nanoparticles via nanoprecipitation. J. Appl. Polym. Sci. 133 (4).

Shalaby, A., Nassef, E., Mubark, A., Hussein, M., 2014. Phosphate removal from wastewater by electrocoagulation using aluminium electrodes. Am. J. Environ. Eng. Sci. 1 (5), 90–98.

Shang, J., Gao, X., 2014. Nanoparticle counting: towards accurate determination of the molar concentration. Chem. Soc. Rev. 43 (21), 7267–7278.

Shen, M., Hu, T., Huang, W., Song, B., Zeng, G., Zhang, Y., 2021. Removal of microplastics from wastewater with aluminosilicate filter media and their surfactant-modified products: performance, mechanism and utilization. Chem. Eng. J. 421, 129918.
Shen, M., Zhang, Y., Almatrafi, E., Hu, T., Zhou, C., Song, B., Zeng, Z., Zeng, G., 2022. Efficient removal of microplastics from wastewater by an electrocoagulation process. Chem. Eng. J. 428, 131161.
Shi, X., Zhang, X., Gao, W., Zhang, Y., He, D., 2022. Removal of microplastics from water by magnetic nano-fe3o4. Sci. Total Environ. 802, 149838.
M. Sillanpää, M. Shestakova, Chapter 2—electrochemical water treatment methods bt—electrochemical water treatment methods. 47–130 (2017).
Song, Y.K., Hong, S.H., Eo, S., Han, G.M., Shim, W.J., 2020. Rapid production of micro-and nanoplastics by fragmentation of expanded polystyrene exposed to sunlight. Environ. Sci. Technol. 54 (18), 11191–11200.
Tsai, M.-H., Chao, S.-J., Chung, K.-H., Hua, L.-C., Huang, C., 2023. Destabilization of polystyrene nanoplastics with different surface charge and particle size by fe electrocoagulation. Sci. Total Environ. 872, 162254.
Vysotskii, V., Uryupina, O., Gusel'nikova, A., Roldugin, V., 2009. On the feasibility of determining nanoparticle concentration by the dynamic light scattering method. Colloid J. 71 (6).
Wang, Y., Li, Y., Tian, L., Ju, L., Liu, Y., 2021. The removal efficiency and mechanism of microplastic enhancement by positive modification dissolved air flotation. Water Environ. Res. 93 (5), 693–702.
Wyatt, P.J., 2018. Measuring nanoparticles in the size range to 2000 nm. J. Nanopart. Res. 20 (12), 1–18.
Xiong, Y., Zhao, J., Li, L., Wang, Y., Dai, X., Yu, F., Ma, J., 2020. Interfacial interaction between micro/nanoplastics and typical ppcps and nanoplastics removal via electrosorption from an aqueous solution. Water Res. 184, 116100.
Zeboudji, B., Drouiche, N., Lounici, H., Mameri, N., Ghaffour, N., 2013. The influence of parameters affecting boron removal by electrocoagulation process. Sep. Sci. Technol. 48 (8), 1280–1288.
Zeng, E.Y., 2018. Microplastic contamination in aquatic environments: an emerging matter of environmental urgency. Elsevier.
Zhang, Y., Jiang, H., Bian, K., Wang, H., Wang, C., 2021. A critical review of control and removal strategies for microplastics from aquatic environments. J. Environ. Chem. Eng. 9 (4), 105463.